Available online at www.sciencedirect.com
ScienceDirect
Trans. Nonferrous Met. Soc. China 30(2020) 1731−1742
Transactions of Nonferrous Metals Society of China
www.tnmsc.cn

# Microstructure, mechanical and wear properties of aluminum borate whisker reinforced aluminum matrix composites

Neeraj PANDEY[1], I. CHAKRABARTY[2], Kalpana BARKANE[1], N. S. MEHTA[1], M. R. MAJHI[1]

1. Department of Ceramic Engineering, Indian Institute of Technology (BHU), Varanasi, U.P., India;
2. Department of Metallurgical Engineering, Indian Institute of Technology (BHU), Varanasi, U.P., India

Received 30 November 2019; accepted 9 May 2020

**Abstract:** The microstructural features and the consequent mechanical properties were characterized in aluminium borate whisker (ABOw) (5, 10 and 15 wt.%) reinforced commercially-pure aluminium composites fabricated by conventional powder metallurgy technique. The aluminium powder and the whisker were effectively blended by a semi-powder metallurgy method. The blended powder mixtures were cold compacted and sintered at 600 °C. The sintered composites were characterized for microstructural features by optical microscopy (OM), scanning electron microscopy (SEM), energy dispersive spectroscopy (EDS), transmission electron microscopy (TEM) and X-ray diffraction (XRD) analysis. Porosity in the composites with variation in ABOw contents was determined. The effect of variation in content of ABOw on mechanical properties, viz. hardness, bending strength and compressive strength of the composites was evaluated. The dry sliding wear behaviour was evaluated at varying sliding distance at constant loads. Maximum flexural strength of 172 MPa and compressive strength of 324 MPa with improved hardness around HV 40.2 are obtained in composite with 10 wt.% ABOw. Further increase in ABOw content deteriorates the properties. A substantial increase in wear resistance is also observed with 10 wt.% ABOw. The excellent combination of mechanical properties of Al−10wt.%ABOw composites is attributed to good interfacial bonds, less porosity and uniformity in the microstructure.

**Key words:** aluminum matrix composite; powder metallurgy; aluminum borate whisker (ABOw) reinforcement; flexural strength; compression test; dry sliding wear

## 1 Introduction

Aluminum matrix composites reinforced with discontinuous whiskers are being widely used in automotive and aerospace fields because of their excellent specific strength, wear resistance and high-temperature durability [1−3]. Various types of ceramic whiskers such as silicon carbide, silicon nitride, aluminium borate, and magnesium di-aluminum tetraoxide (spinels) are used as reinforcements. Among them, aluminium borate whisker (ABOw) is an attractive reinforcement for aluminium and alloy matrix composites due to its excellent mechanical properties like elastic modulus, strength and creep resistance. At the same time, ABOw is much cost-effective compared to other ceramic whiskers [4−6].

Metal matrix composites are generally fabricated by two different routes, either by casting process or by powder metallurgy. The casting processes offer several advantages like ease of fabrication of complex shapes in a cost-effective way and being most suited for mass production of components. However, the casting route suffers from excessive reinforcement/matrix interface reaction and poor wettability of the ceramic reinforcing phase in the metal matrix. These demerits of casting route can be overcome by powder metallurgy route.

**Corresponding author:** Neeraj PANDEY; Tel: +91-9236119762; E-mail: neerajp.rs.cer16@itbhu.ac.in
DOI: 10.1016/S1003-6326(20)65334-1

The whisker/matrix interface plays a vital role in determining the ultimate properties of the composites. Aluminium alloy matrix containing Mg is prone to such type of interfacial reaction leading to the deterioration of mechanical properties [7−14]. Hence, to reduce interfacial reactions and to improve the wettability, ABOw whiskers are coated with different types of substances and the resulting properties are evaluated [4−6,8−11,14]. However, with pure aluminum matrix, the interfacial reaction has been less reported [15]. CHU et al [16] reported that the interfacial reaction took place in the specimens with prolonged exposure at 500 °C for 50 h; $\gamma$-$Al_2O_3$ phases with the spinel structure and boron are produced; Elastic modulus, ultimate tensile strength as well as yield strength initially increased, and then decreased with time at 500 °C.

The ABOw reinforced aluminium alloy matrix composites are so far reported to be fabricated mostly via liquid metallurgy route specifically by squeeze casting process except a very few via powder metallurgy route [17,18]. In view of this, the present investigation was undertaken to characterize the microstructural features and mechanical properties developed in pure Al−ABOw composite fabricated by conventional powder metallurgy technique by blending, cold compaction and sintering.

## 2 Experimental

Aluminium borate whiskers were synthesized by hydrolysis method and calcined at 1300 °C [19]. Pure aluminum metal powder of 99.5% in purity and particle size of 20−40 μm was used as a matrix and procured from Poly-Chem Private India Limited, Bangalore. For effective dispersion of the ABOw whiskers in the matrix, a simple method was adopted by the semi-powder metallurgy method [20]. The constituent powders were mixed in non-reactive solvent instead of ball milling. Al powder was vigorously mixed with ethanol with magnetic stirring for 40 min, and then ABOw was added in varying contents of 5, 10 and 15 wt.% at 80 °C in vacuum and stirred for another 15 min. After hydrolysis sol was dried in oven at 110 °C in vacuum for 4 h, dried sol was then mixed with PVA (polyvinyl alcohol) solution and at last the pellet was pressed with the hydraulic press at 180 MPa. Rectangular specimens with the dimensions of 50 mm × 10 mm × 10 mm for flexural strength, cylindrical specimens with the dimensions of 30 mm (length) × 8 mm (diameter) for wear tests and cylindrical specimens with the dimensions of 20 mm (length)×15 mm (diameter) for compression tests were sintered in argon gas environment in a sintering furnace. The heating rate was 5 °C/min to raise the temperature to 600 °C and soaked for 2 h and subsequently cooled to room temperature.

For detection of phases in the sintered composites, X-ray diffraction analysis was carried out in Rigaku Smart Lab at 40 kV and 15 mA using Cu $K_\alpha$ ($\lambda$=0.154 nm) radiation. The microstructural features were observed under an optical microscope (Leitz) adopting conventional methods of sample preparation. The polished samples were etched with Keller's reagent. Composite microstructures and reinforcement morphologies were further examined using scanning electron microscope (SEM) ZEISS EVO 18 operating at 20 kV. Reinforcement/matrix interface characteristics and crystal structures of ABOw reinforcement were examined under the transmission electron microscope (TECHNAI $G^2$ T20) operated at 200 kV. Instron−5848 was used for evaluation of compressive strength with a crosshead speed of 0.15 mm/min (corresponding to engineering strain rate of $1\times10^{-3}$ $s^{-1}$). Densities of the composites were determined by Archimedes' immersion method following ASTM C20 specification. The flexural strength is measured by a universal testing machine using Tinius Olsen (H10KL). Bending strength ($S_B$) was calculated using the following expression:

$$S_B = \frac{3FL}{2wt^2} \quad (1)$$

where $F$ is the load at failure, $L$ is the distance between the supports, $w$ is the sample width, and $t$ is the thickness of the sample.

Dry sliding wear behavior of the Al−ABOw composites were evaluated using a pin-on-disc type tribometer (DUCOM, TL−20) with a data acquisition system, against a standard disc of hardened high-carbon chromium steel counter face (HRC 64) with surface roughness ($R_a$) of 0.511 μm. Scanning probe microscope (SPM) (model NTEGRA prima) was used to measure the surface roughness of composites. Dry sliding wear tests

were performed with varying sliding distance at room temperature under a normal load of 10 N and a fixed velocity of 1.15 m/s. The mass loss of samples was measured with digital balance (least count 0.1 mg).

## 3 Results and discussion

### 3.1 Microstructural characterization and phase identification

3.1.1 Morphology of ABOw

The average diameters of the whiskers are observed to range from 0.3 to 0.8 μm (Fig. 1). It is difficult to separate the whiskers from the bulk due to the moderately high bonding strength among the whiskers. So, the exact measurement of the accurate length is not possible. However, the approximate aspect ratio of the length to diameter of whiskers is pretty high, about 15−20. The whisker thickness is relatively homogeneous for each material. This morphology confirms aluminum borate and is substantiated by the XRD analysis. Figure 2 shows

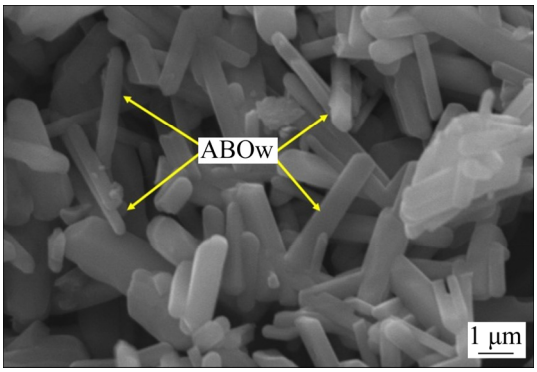


**Fig. 1** SEM image of ABOw calcined at 1300 °C used as reinforcement

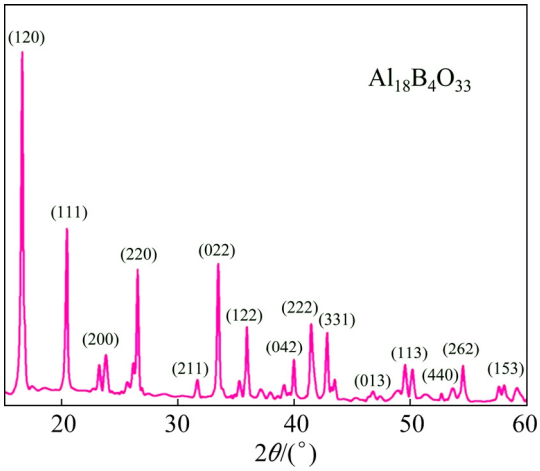


**Fig. 2** XRD pattern of ABOw calcined at 1300 °C

the XRD patterns of the ABOw calcined at 1300 °C. The identified diffracted peaks correspond to aluminum borates ($Al_{18}B_4O_{33}$).

The TEM bright field images with corresponding diffraction patterns of ABOw powder prepared by the hydrolysis method are shown in Fig. 3. The morphological and discontinuous structure of the micro whiskers is characterized and the crystal parameters are determined to be $a$=7.6874 Å, $b$=15.0127 Å and $c$=5.6643 Å. The parameters confirm the orthorhombic crystal structure of ABOw reinforcements [21].

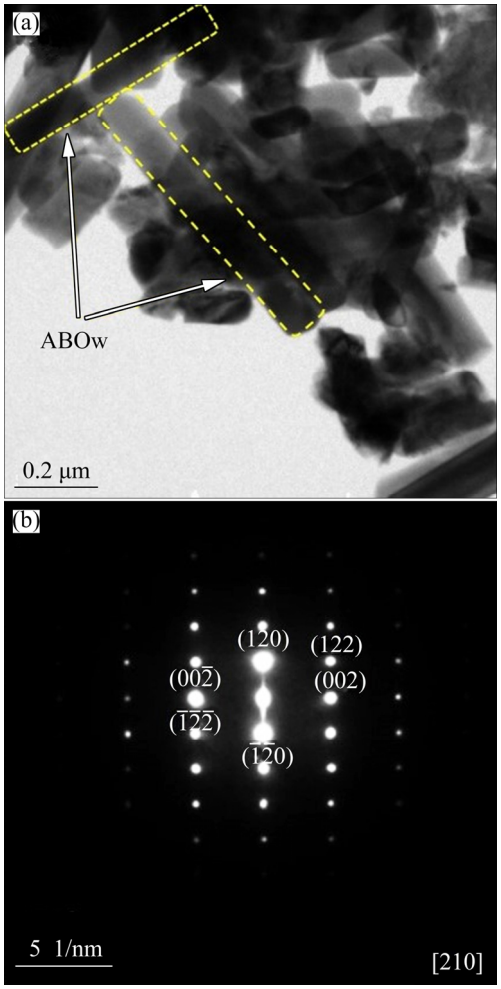


**Fig. 3** TEM bright field image (a) and corresponding SAED (b) of ABOw

3.1.2 Microstructural characterization of composites

The scanning electron micrographs of base metal and composites are shown in Fig. 4. The scanning electron micrographs show almost uniform distributions of ABOw throughout the volume of the composites.

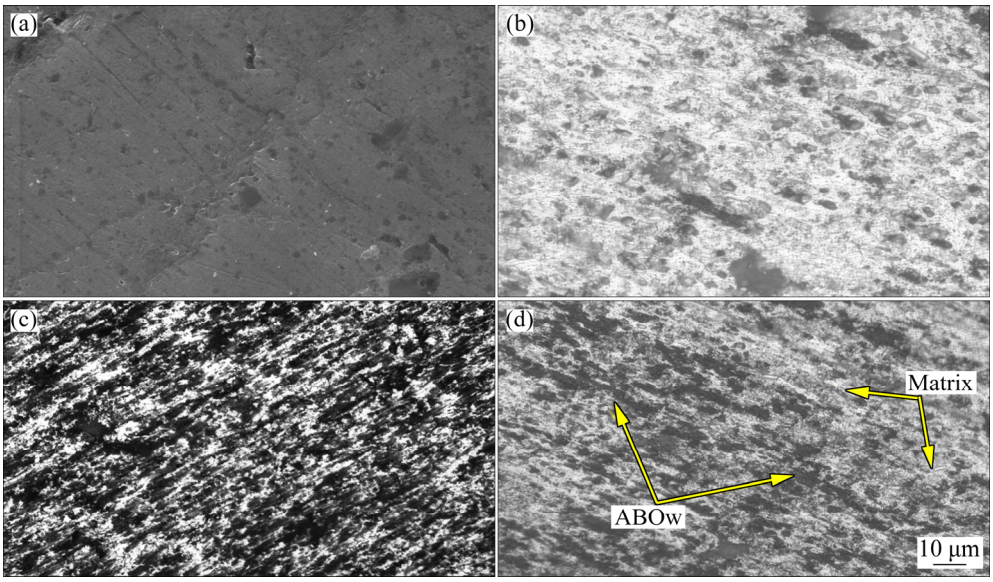


**Fig. 4** SEM micrographs of aluminum base metal (a) and Al−ABOw composite with 5 wt.% (b), 10 wt.% (c) and 15 wt.% (d) ABOw

It is evident from the XRD patterns (Fig. 5) of the composites that, except aluminium and $Al_{18}B_4O_{33}$ type of aluminium borate whiskers, no other phases are present in the fabricated composites. This confirms the absence of any whisker/matrix interface reaction during sintering of the cold compacts. Similar observation has been reported earlier by YAO et al [15]. As the mass fraction of ABOw increases, intensity of ABOw peaks increases whereas that of aluminium peaks decreases.

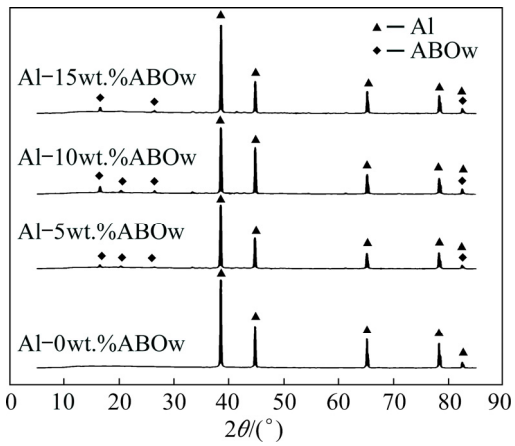


**Fig. 5** XRD patterns of sintered Al−ABOw composites with different compositions

### 3.2 Measurement of density and porosity

The average porosities of the Al−ABOw composites with varying contents of ABOw are calculated from experimentally determined densities and theoretical densities and are listed in Table 1. Although ABO whiskers have densities of 2.94 g/cm$^3$, a little bit higher than that of aluminum (2.67 g/cm$^3$), with increasing content of ABOw, the composite densities decrease. This is due to more porosities incorporated with higher volume of ABOw. It is evident from the Table 1 that, the average porosity increases with increasing content of ABOw.

### 3.3 Evaluation of mechanical properties

3.3.1 Vickers hardness and bending strength

The hardness values of Al base metal and the Al−ABOw composites are given in Table 2. The hardness of the composites is observed to increase with increasing the content of ABO whiskers in the composites. This may be due to the inhibition of the progress of plastic deformation by whiskers present in the matrix. However, with the increase in porosity, the actual hardness values are over-shadowed and as a result, the hardness in composite with 15 wt.% ABOw is reduced. As the agglomeration of whiskers proceeds in specimens with 15 wt.% ABOw, the non-uniform sintering driving force leads to localized shrinkage strains introducing more defects (dislocations and point defects, etc) at the interfaces of ABOw and matrix during grain growth so that the interface strength decreases during sintering. This behavior of

**Table 1** Densities and porosities of composite samples

| Content of ABOw/ wt.% | No. | Experimental density/ ($g \cdot cm^{-3}$) | Theoretical density/ ($g \cdot cm^{-3}$) | Average porosity/ % |
|---|---|---|---|---|
| 0 | 1 | 2.56 | 2.70 | 5.43 |
| | 2 | 2.53 | | |
| | 3 | 2.58 | | |
| 5 | 1 | 2.47 | 2.65 | 7.48 |
| | 2 | 2.48 | | |
| | 3 | 2.45 | | |
| 10 | 1 | 2.32 | 2.61 | 11.17 |
| | 2 | 2.30 | | |
| | 3 | 2.29 | | |
| 15 | 1 | 2.30 | 2.57 | 12.86 |
| | 2 | 2.28 | | |
| | 3 | 2.27 | | |

**Table 2** Bending strength and Vickers hardness of samples

| Content of ABOw in composites/wt.% | Bending strength at room temperature/MPa | Hardness (HV) |
|---|---|---|
| 0 | 125±2 | 27 |
| 5 | 160±2 | 37 |
| 10 | 172±2 | 40 |
| 15 | 165±2 | 39 |

composite increases with increasing volume fraction of defects in aluminum matrix [19,22]. The flexural strength of the samples were calculated using three-point bending test, with a span of 30 mm and a crosshead speed of 0.5 mm/min (Table 2). A linear increase of bending strength can be observed up to Al−10wt.%ABOw (172 MPa) but drops with a further increase in content of ABOw to 15 wt.% due to the brittleness of the whiskers and higher porosity. Hence, it can be inferred that the bending strength increases as a result of increase in strength by dispersion strengthening.

3.3.2 Compression behaviour

The behavior of composites under compression is shown in the engineering stress−strain diagram in Fig. 6. The maximum compressive strength (324 MPa) can be observed in composite having 10 wt.% ABOw while with decreasing the content of ABOw the compressive strength (217 MPa) decreases. However, excess ABOw reduces compressive strength due to the agglomeration of brittle ABOw as evident with 15 wt.% addition of ABOw. The macrographs exhibiting compressive surface failures of composites with different contents of ABOw at room temperature are shown in Fig. 7. Numerous longitudinal surface cracks can be observed on the surface as the content of ABOw is increased.

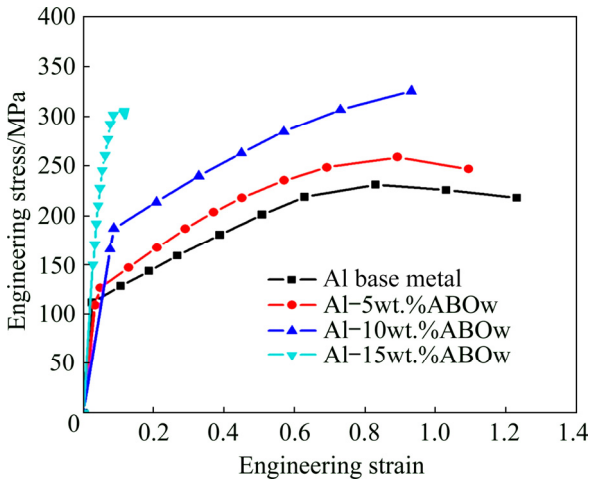


**Fig. 6** Engineering stress−strain curves of base metal and composites with different contents of reinforcements

### 3.4 Fracture characteristics

3.4.1 Fractography of bending failures

The typical SEM fractographs of Al−ABOw composites are exhibited in Fig. 8. Aluminium base metal fractures without any whisker reinforcement, exhibiting ductile nature; the fracture propagates along the micro holes and dimples on the surface. In contrast, the fracto-graphy of Al/ABOw composites in Fig. 8(a) depicts predominantly brittle nature of fracture. But, most of the whiskers remain intact in the matrix and are not dislodged from the matrix. So, it can be inferred that the matrix can transfer the load efficiently through the interfaces to the whiskers without being dislodged from the matrix. Consequently, enhanced mechanical properties are observed in this composite up to an ABOw content of 10 wt.%. The whiskers are more or less evenly dispersed in the matrix. However, in the composite with 15 wt.% of ABOw, dispersion is not so uniform, as revealed at very high magnification; clusters of whiskers are present at different locations. This leads to a decrease in bending strength in the composite with 15 wt.% ABOw.

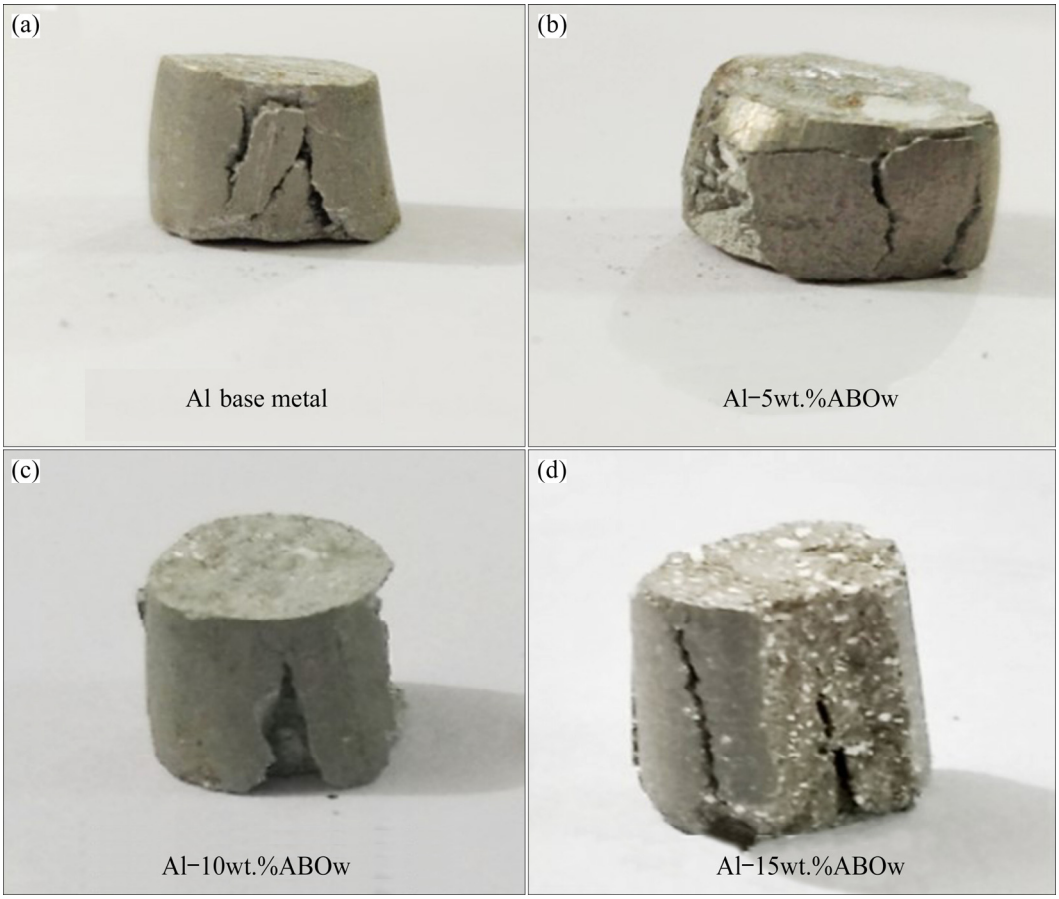


**Fig. 7** Macrographs showing longitudinal surface cracks during compressive failure of aluminium base metal (a) and sintered Al−ABOw composites (b−d)

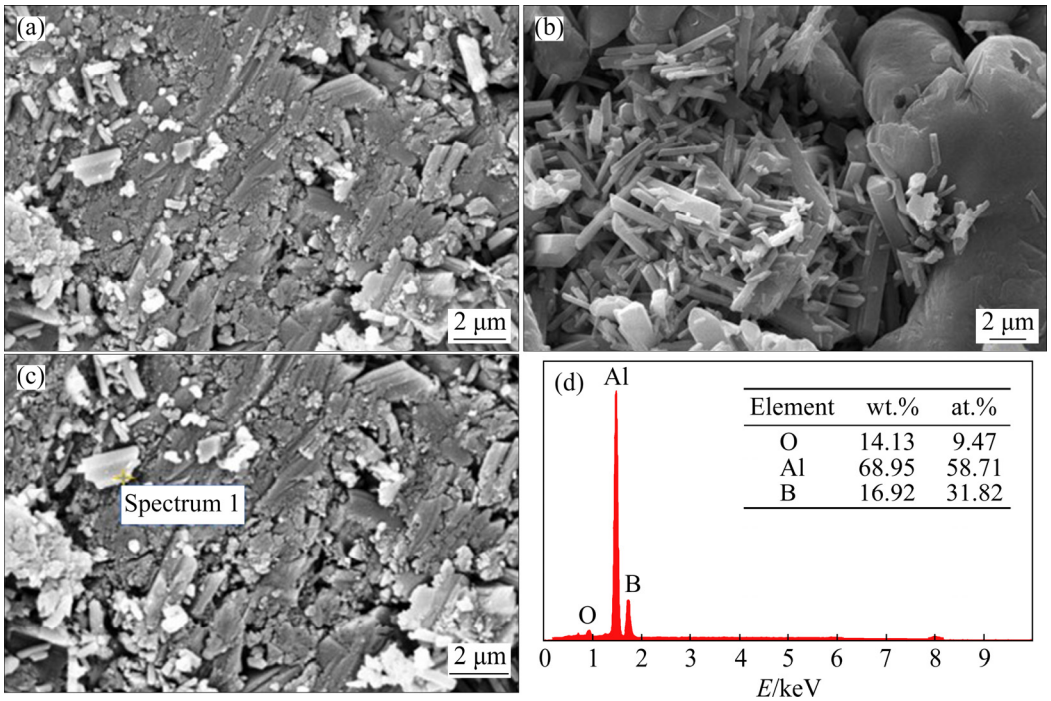


**Fig. 8** Typical fractographs in bending test: (a) Al−10wt.%ABOw; (b) Al−15wt.%ABOw; (c) EDS analysis point of Al−10wt.%ABOw; (d) EDS spectrum from dislodged ABOw

3.4.2 Fractography of compressive failures

The fractographs of compressive failures of composites at low magnifications are shown in Fig. 9. The compression in aluminum base sample is ductile in nature as compared to other specimens. With increase in the content of ABOw (15 wt.%), the fracture is more brittle in nature. The characteristic of groove with many microvoids which contributes to the motion of whisker to a certain extent can be observed, as shown in Fig. 9(d). Certainly, the ABOw is inclined to crack caused by high local stress in turn. With the higher content of ABOw, the proportion of the region representing the flow localization increases and the matrix has to accommodate the deformation between the region of plasticity and non-plasticity. Consequently, damage would be caused by plasticity instability. This can be manifested by the secondary crack, as shown in Fig. 9(d). The occurrence of localized plasticity signifies the improvement of the plastic deformation capacity; nevertheless, the whole deformation process shows typical characteristics of brittle fracture. Figure 10 shows the SEM fractrography at higher magnifications and ABOw is clearly seen on the fracture surface. Some fragmentation of whiskers to smaller sizes is noticed in the samples specifically with 15 wt.% ABOw.

### 3.5 Strengthening mechanisms

The combined effects of various strengthening mechanisms, namely load transfer, thermal mismatch, and Orowan strengthening improve the ultimate strength of the composites.

The transfer of external load from matrix to reinforcements depends on the volume fraction of reinforcements and the matrix/reinforcements interface bonding. The change in compressive strength due to load transfer ($\Delta\sigma_{load}$) can be expressed as

$$\Delta\sigma_{load}=\frac{1}{2}\sigma_m V_f[s\theta+\frac{3\pi-4}{3\pi}(1+\frac{1}{s})\theta] \quad (2)$$

where $\theta$ is the angle between the whisker orientation and the compression direction (average angle can be considered as $\pi/4$), $\sigma_m$ is the yield strength of Al matrix, $V_f$ is the volume fraction of whiskers, and $s$ is the average aspect ratio of ABO whiskers.

The mismatch between the coefficient of thermal expansion of whisker and the aluminium matrix causes high dislocation density during cooling from the sintering temperature to room temperature. The resultant high dislocation density is expressed as

$$\rho_t=\frac{BV_f(\alpha_m-\alpha_f)\Delta T}{b(1-V_f)d} \quad (3)$$

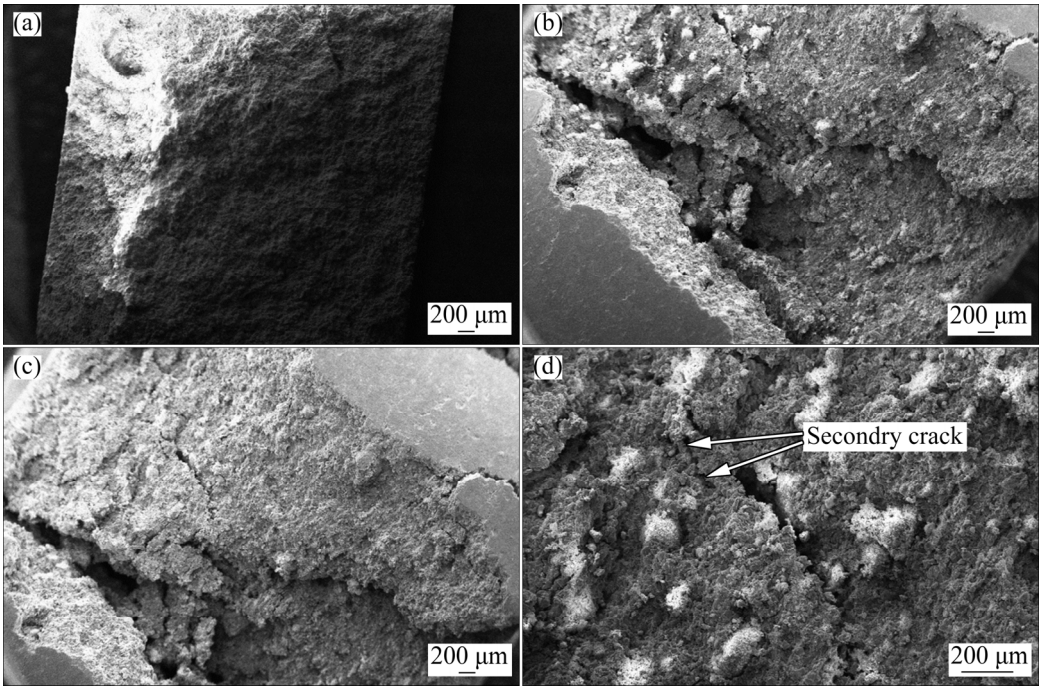


**Fig. 9** Fractographs at low magnification of aluminium base metal (a) and composites with 5 wt.% (b), 10 wt.% (c) and 15 wt.% (d) ABOw

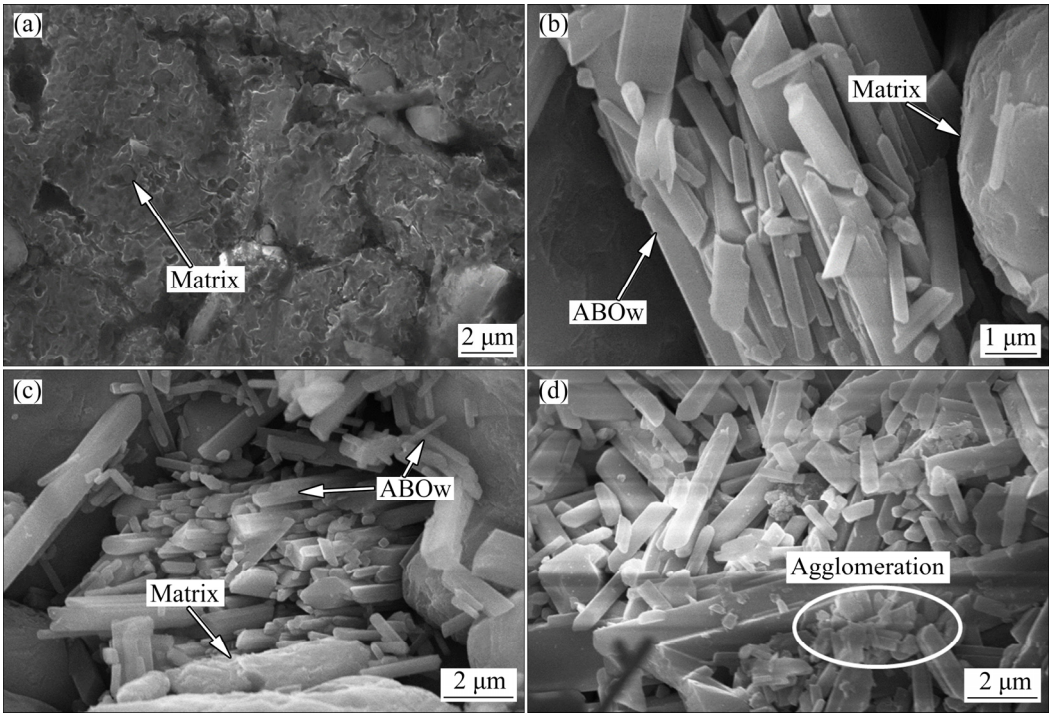


**Fig. 10** Fractographs at higher magnification of base aluminium (a) and composites with 5 wt.% (b), 10 wt.% (c) and 15 wt.% (d) ABOw

where $B$ is a geometrical constant and is equal to 10 for whiskers; $b$ is the absolute value of Burger vector and is equal to 2.86 nm; $\alpha_m$ and $\alpha_f$ are the coefficients of thermal expansion of matrix and whisker, respectively, and the values are $23.6\times10^{-6}$ and $2.6\times10^{-6}$ $K^{-1}$; $d$ is the minimum size of the whiskers (0.5 μm); $\Delta T$ is the difference between sintering temperature and room temperature.

Hence, the combined effect of dislocation densities is

$$\Delta\sigma_D = \lambda G_m b\sqrt{\rho_t} \quad (4)$$

where $\lambda$ is a constant and is equal to 1.25, and $G_m$ is shear modulus equal to 27 GPa.

The ultimate compressive yield strength ($\Delta\sigma$) can be evaluated from the relationship:

$$\Delta\sigma = \sqrt{\Delta\sigma_{load}^2 + \Delta\sigma_D^2} \quad (5)$$

The estimated combined yield strengths of the Al−ABOw composites with varying contents of ABOw are presented in Table 3. It is evident that, the estimated compressive yield strengths widely differ from the actual results. This is perhaps due to the agglomeration of whiskers at locations with increasing content of ABOw.

**Table 3** Theoretical estimation of different strengthening effects

| Content of ABOw/ wt.% | Strengthening due to load transfer, $\Delta\sigma_{Load}$/MPa | Strengthening due to dislocation, $\Delta\sigma_D$/MPa | Total theoretical yield strength, $\Delta\sigma$/MPa |
|---|---|---|---|
| 5 | 119 | 140 | 184 |
| 10 | 356 | 108 | 372 |
| 15 | 415 | 133 | 434 |

### 3.6 Dry sliding wear behaviour

The wear rate versus sliding distance (time) of different Al−ABOw composites under fixed normal load (10 N) and sliding velocity (1.15 m/s) are shown in Fig. 11. The wear rate of Al−ABOw composites decreases with increase in ABOw content up to 10 wt.%. However, further increase in ABOw content results in an increased wear rate. Up to about 10 wt.%, the whiskers are more or less randomly distributed in the matrix and the matrix/ reinforcement interface has adequate strength to combat the wear. But the excess content of ABOw leads to a non-uniform dispersion and clusters form. These clusters of whiskers are easily dislodged during wear because of their weak matrix/ reinforcement interface strength. The dislodged

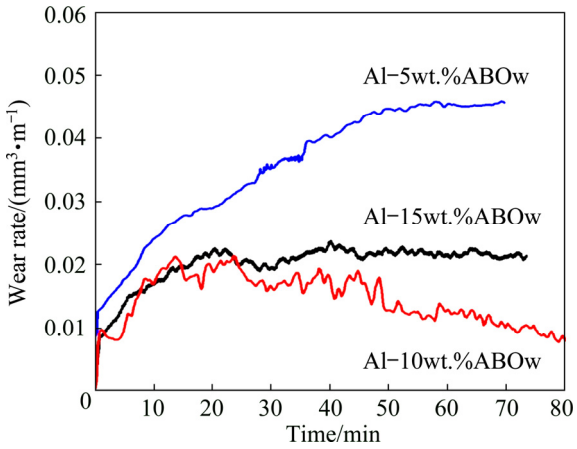


**Fig. 11** Variation in wear rate with sliding distance (time) for different contents ABOw reinforced Al matrix composites

whiskers cause a three-body abrasion with further sliding of the mating surfaces. At the initial period of sliding, both 10 wt.% and 15 wt.% ABOw reinforced composites show almost same wear rate but as the sliding progresses, the frictional heat generated increases. The increased contact surface temperature leads to softening of the matrix and this in turn raises the degree of plastic deformation which aggravates the dislodging of whiskers from the matrix.

The worn surface topographs under SEM at maximum sliding distance traversed are shown in Fig. 12. It can be seen that, the fragmentation of asperities, the formation of wear debris and cracks and the delaminations are prominent. In base metal and composite with 5 wt.% ABOw, the sliding grooves are deeper because of the plowing action of the hard steel surface asperities on softer test sample surface. Worn surface of Al−10wt.%ABOw composite is much smoother and almost free form wear debris. However, with 15 wt.% ABOw, shallow surface scars with fine cracks and subsequent delamination are observed. The cracks propagate both in longitudinal and transverse directions with respect to sliding direction. The 2D and 3D profile analysis of the worn surfaces and the surface roughness values are shown in Figs. 13 and 14, respectively. The wear scar characteristics substantiate the SEM observations. The surface roughness is the minimum with 10 wt.% ABOw and increases a little bit with 15 wt.% ABOw.

The observed coefficients of friction (COF) in Al−ABOw composites are shown in Fig. 15. It is evident that, the average COF values are almost similar in composites with 5 and 10 wt.% ABOw. However, in composite with 15 wt.% ABOw, there is substantial increase in COF value. In the case of 15 wt.% ABOw composite, the dislodged whiskers by the shearing action are adhered in between the two mating surfaces increasing the COF.

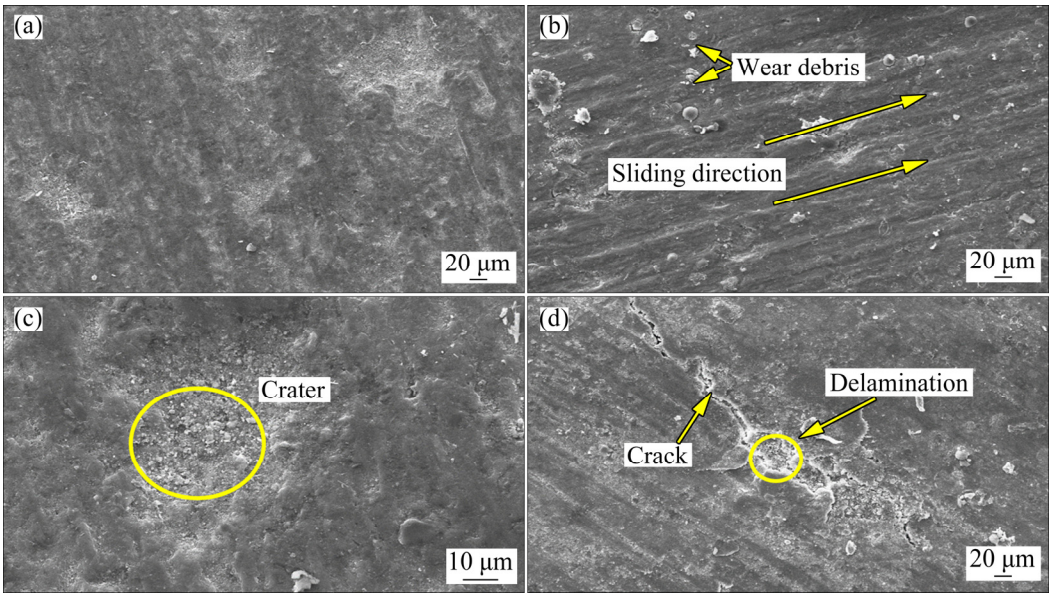


**Fig. 12** SEM images of worn surfaces of aluminium base metal (a) and composites with 5 wt.% (b), 10 wt.% (c) and 15 wt.% (d) ABOw

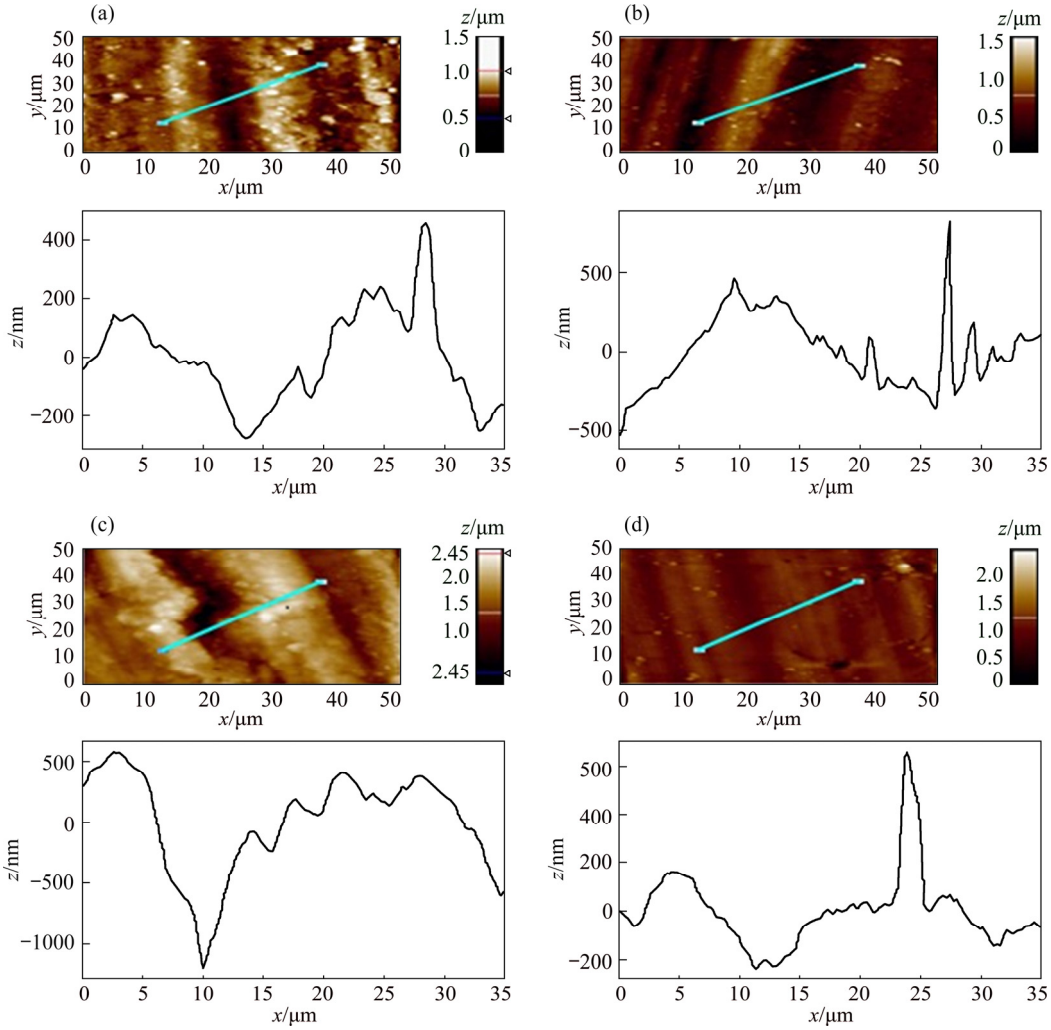


**Fig. 13** Line analysis results perpendicular to wear track and 2D-profilometric images of aluminium base metal (a) and composites with 5 wt.% (b), 10 wt.% (c) and 15 wt.% (d) ABOw

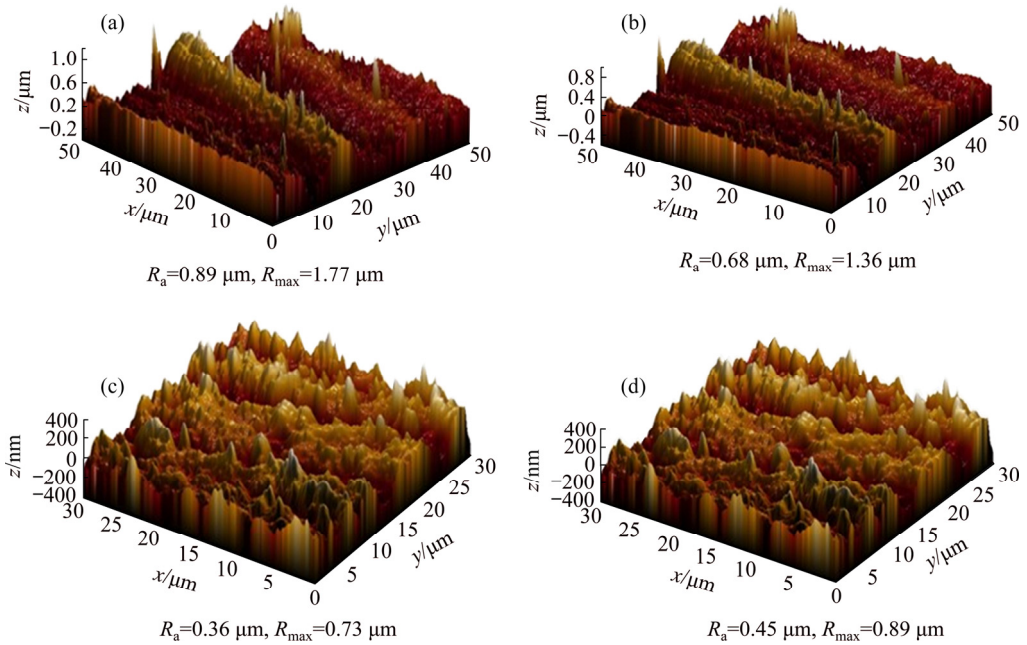


**Fig. 14** 3D-profilometric images of aluminum base metal (a) and composites with 5 wt.% (b), 10 wt.% (c) and 15 wt.% (d) ABOw

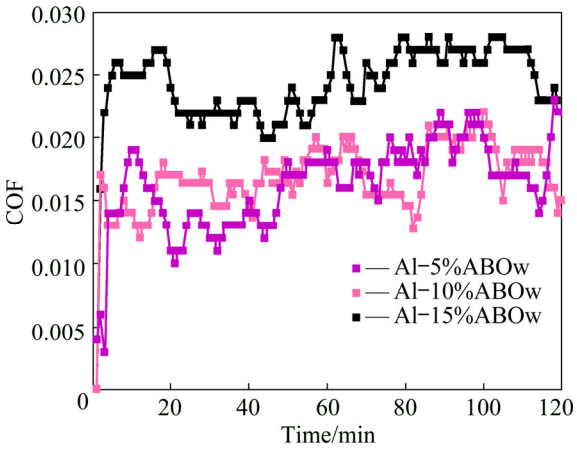


**Fig. 15** Effect of sliding distance (time) on coefficient of friction for different contents ABOw reinforced composites

## 4 Conclusions

(1) The ABO short fibres are more or less uniformly dispersed in the matrix up to a whisker mass fraction of 10%, but further increase in whisker content leads to clustering at different places. There is no sign of matrix/whisker interface reaction after sintering of green compacts at 600 °C.

(2) The density of the composite decreases with increasing content of whisker in the matrix due to the increase in porosity with increasing content of whisker.

(3) The hardness of composites increases up to 10 wt.% ABOw addition due to dispersion strengthening with reduced porosity and more interfacial bonding between matrix and reinforcement. With 15 wt.% ABOw, the effect of whisker strengthening is overshadowed by porosity leading to a reduction in hardness and strength.

(4) The flexural strength of around 172 MPa and compression strength of 324 MPa with 10 wt.% ABOw reinforcement are observed due to lower porosity and better reinforcement dispersion than other sintered samples.

(5) Al−10wt.%ABOw exhibits the best dry sliding wear resistance. With 15 wt.% ABOw, the whiskers are dislodged due to non-uniform dispersions forming larger quantities of debris.

(6) From microstructural characterization and the mechanical properties developed in the Al−ABOw composites, it can be inferred that 10 wt.% whisker is optimum to yield the best ultimate properties.

## Acknowledgments

The authors gratefully acknowledge the support provided by the Central Instrument Facility Centre (CIFC) of IIT (BHU) and the Department of Ceramic Engineering especially Advance Refractory Lab (ARL) of IIT (BHU) Varanasi.

## References

[1] ZHU S J, IIZUKA T. Fatigue behaviour of $Al_{18}B_4O_{33}$ whisker-framework reinforced Al matrix composites at high temperatures [J]. Composite Science and Technology, 2003, 63: 265−271.

[2] YU Z Y, ZHAO N Q, LIU E Z, SHI C S, DU X W, WANG J. Fabrication of aluminum matrix composites with enhanced mechanical properties reinforced by in situ generated $MgAl_2O_4$ whiskers [J]. Composite Part A: Applied Science and Manufacturing, 2012, 43: 631−634.

[3] GUO C, ZOU T C, SHI C S, YANG X D, ZHAO N Q, LIU E Z, HE C N. Compressive properties and energy absorption of aluminum composite foams reinforced by in-situ generated $MgAl_2O_4$ whiskers [J]. Materials Science and Engineering A, 2015, 645: 1−7.

[4] ZHAO P T, WANG L D, DU Z M, XU S C, JIN P P, FEI W D. Low temperature extrusion of 6061 aluminum matrix composite reinforced with $SnO_2$-coated $Al_{18}B_4O_{33}$ whisker [J]. Composite Part A: Applied Science and Manufacturing, 2012, 43: 183−188.

[5] LIU G, REN W C, SUN Y L, HU J. Damping behaviour of $Bi_2O_3$-coated $Al_{18}B_4O_{33}$ whisker-reinforced pure Al composite [J]. Materials Science and Engineering A, 2010, 527: 5136−5142.

[6] YU Y C, TANG S W, WANG Z L, HU J. Effects of coating contents on the copper-coated $Al_{18}B_4O_{33}$ whisker reinforced 6061Al composite [J]. Materials Science and Engineering A, 2008, 479: 261−268.

[7] WANG Z L, TANG S W, YU Y C, HU J. The effects of Mg contents on microstructure and tensile properties of $Al_{18}B_4O_{33}$w/Al−Mg composites [J]. Journal of Alloys and Compounds, 2019, 779: 404−411.

[8] LIU G, TANG S W, REN W C, HU J. Effect of thermal cycling on the damping behaviour in alumina borate whisker with and without $Bi_2O_3$ coating reinforced pure aluminium composites [J]. Materials Design, 2014, 60: 244−249.

[9] YUE Y H, WANG B, GAO X, ZHANG S L, LIN X Y, YAO L H, GUO E J. Effect of interfacial modifying on the microstructures, mechanical properties and abrasive wear properties of aluminum borate whiskers reinforced 6061Al composite [J]. Journal of Alloys and Compounds, 2017, 25: 395−402.

[10] DING D Y, WANG D Z, ZHANG W L, YAO C K, LI D X. Interfacial reactions and mechanical properties of 6061Al matrix composites reinforced with alumina coated $Al_{18}B_4O_{33}$ whiskers [J]. Materials Letters, 2000, 45: 6−11.

[11] HE H Y, GUO E J, FEI W D, WANG L P. Tensile properties and thermal stability of ZnO-coated aluminum borate

whiskers reinforced 2024Al composite [J]. Materials Science and Engineering A, 2011, 528: 2407−2411.
[12] HU J, ZHANG J X, TANG S W, REN W C. Effect of annealing treatment on microstructure and tensile strength of alumina borate whisker-reinforced Al−Mg composite [J]. Materials Science and Engineering A, 2006, 433: 94−99.
[13] PARK H Y, PARK M I, CHO M K, OAK J J, KIMURA H. Mechanical properties of squeeze infiltrated AS52 magnesium matrix composites [J]. International Journal of Modern Physics B, 2009, 23: 1510−1515.
[14] SASAKIA G, WANGA W G, HASEGAWAA Y, CHOIA B Y, FUYAMAB N, MATSUGIA K, YANAGISAWA O. Surface treatment of $Al_{18}B_4O_{33}$ whisker and development of $Al_{18}B_4O_{33}$/ZK60 magnesium alloy matrix composite [J]. Journal of Materials Processing Technology, 2007, 187−188: 429−432.
[15] YAO L J, SASAKI G, FUKUNAGA H. Reactivity of aluminum borate whisker reinforced aluminum alloys [J]. Materials Science and Engineering A, 1997, 225: 59−68.
[16] CHU W G, FEI W D, YANG W, YAO C K. Effect of thermal exposure on interface and tensile properties of aluminum borate whisker reinforced pure aluminium composite [J]. Materials Chemistry and Physics, 2001, 68: 56−61.
[17] MA Z Y, PAN J, NING X G, LI J H, LU X Y, BI J X. Aluminium borate whisker reinforced Al−8.5Fe−l.3V−1.7Si composite [J]. Journal of Materials Science Letters, 1994, 13: 1731−1732.
[18] YU Z Y, ZHAO N Q, LIU E Z, SHI C S, DU X W, WANG J. Low-temperature synthesis of aluminum borate nano whiskers on the surface of aluminum powder promoted by ball-milling pre-treatment [J]. Powder Technology, 2011, 212: 310−315.
[19] PANDEY N, CHAKRABARTY I, SINGH P, MAJHI M R. Effect of sintering temperature on microstructure and flexural strength of alumina borate whisker [J]. Materials Research Express, 2019, 6: 105210.
[20] RASHAD M, PAN F S, ASIF M. Room temperature mechanical properties of Mg−Cu–Al alloys synthesized using powder metallurgy method [J]. Materials Science and Engineering A, 2015, 644: 129−136.
[21] WANG J, SHA J, YANG Q, WANG Y W, YANG D R. Synthesis of aluminium borate nanowires by sol–gel method [J]. Materials Research Bulletin, 2005, 40: 1551−1557.
[22] MEHTA S N, PANDEY C J, PANDEY NEERAJ, PYARE R, MAJHI R M. Developing a high strength physico-mechanical and electrical properties of ceramic porcelain insulator using zirconia as an additive [J]. Materials Research Express, 2018, 57: 075202.

# 硼酸铝晶须增强铝基复合材料的显微组织、力学性能和磨损性能

Neeraj PANDEY[1], I. CHAKRABARTY[2], Kalpana BARKANE[1], N. S. MEHTA[1], M. R. MAJHI[1]

1. Department of Ceramic Engineering, Indian Institute of Technology (BHU), Varanasi, U.P., India;
2. Department of Metallurgical Engineering, Indian Institute of Technology (BHU), Varanasi, U.P., India

**摘　要：**通过传统的粉末冶金技术制备不同含量硼酸铝晶须(ABOw)(5%, 10%, 15%, 质量分数)增强的商业纯铝基复合材料，并对其显微组织特征和力学性能进行研究。采用粉末冶金方法有效混合铝粉和 ABOw，将混合粉冷压后在 600 °C 下烧结。通过光学显微镜(OM)、扫描电子显微镜(SEM)、能谱分析(EDS)、透射电子显微镜(TEM)和 X 射线衍射(XRD)对烧结后的复合材料进行显微组织表征，测定复合材料的孔隙率随 ABOw 含量的变化，研究 ABOw 含量变化对复合材料的力学性能，包括硬度、抗弯强度和抗压强度的影响，及复合材料在恒定载荷下、不同滑动距离下的干滑动磨损行为。结果表明，当 ABOw 含量为 10%(质量分数)时，复合材料具有最大的抗弯强度和抗压强度，分别为 172 MPa 和 324 MPa，并且硬度得到改善，约为 HV 40.2。但是，随着 ABOw 含量的进一步增加，性能降低。含 10%ABOw 复合材料的耐磨性能也得到显著提高。Al−10% ABOw 复合材料优异的综合性能归因于其具有良好的界面结合性能、低的孔隙率和好的组织均匀性。

**关键词：**铝基复合材料；粉末冶金；硼酸铝晶须增强相；抗弯强度；压缩试验；干滑动磨损

**(Edited by Bing YANG)**